3D-Printed PLA/PEO Blend as Biodegradable Substrate Coating with $CoCl_2$ for Colorimetric Humidity Detection

Nattanicha Chaiya[a,b,c], *Donraporn Daranarong*[d], *Patnarin Worajittiphon*[a,b], *Runglawan Somsunan*[a], *Puttinan Meepowpan*[a,b], *Adisorn Tuantranont*[e], *Nawasit Rakbamrung*[f], *Paul D. Topham*[g], *Brian J. Tighe*[g], *Anisa Mahomed*[g] *and Winita Punyodom*[a,b,h]

[a)] *Department of Chemistry, Faculty of Science, Chiang Mai University, Chiang Mai 50200, Thailand*

[b)] *Department of Chemistry and Center for Innovation in Chemistry, Faculty of Science, Chiang Mai University, Chiang Mai 50200, Thailand*

[c)] *Graduate School, Chiang Mai University, Chiang Mai 50200, Thailand*

[d)] *Science and Technology Research Institute, Chiang Mai University, Chiang Mai 50200, Thailand*

[e)] *National Security and Dual-Use Technology Center, National/Science and Technology Development Agency, Pathumthani 12120, Thailand*

[f)] *Department of Chemistry, Faculty of Science, Burapha University, Chon Buri, 20131, Thailand*

[g)] *Aston Institute of Materials Research, College of Engineering and Physical Sciences, Aston University, Birmingham, United Kingdom*

[h)] *Center of Excellence in Materials Science and Technology, Chiang Mai University, Chiang Mai 50200, Thailand*

*Corresponding Author's E-mail: winitacmu@gmail.com

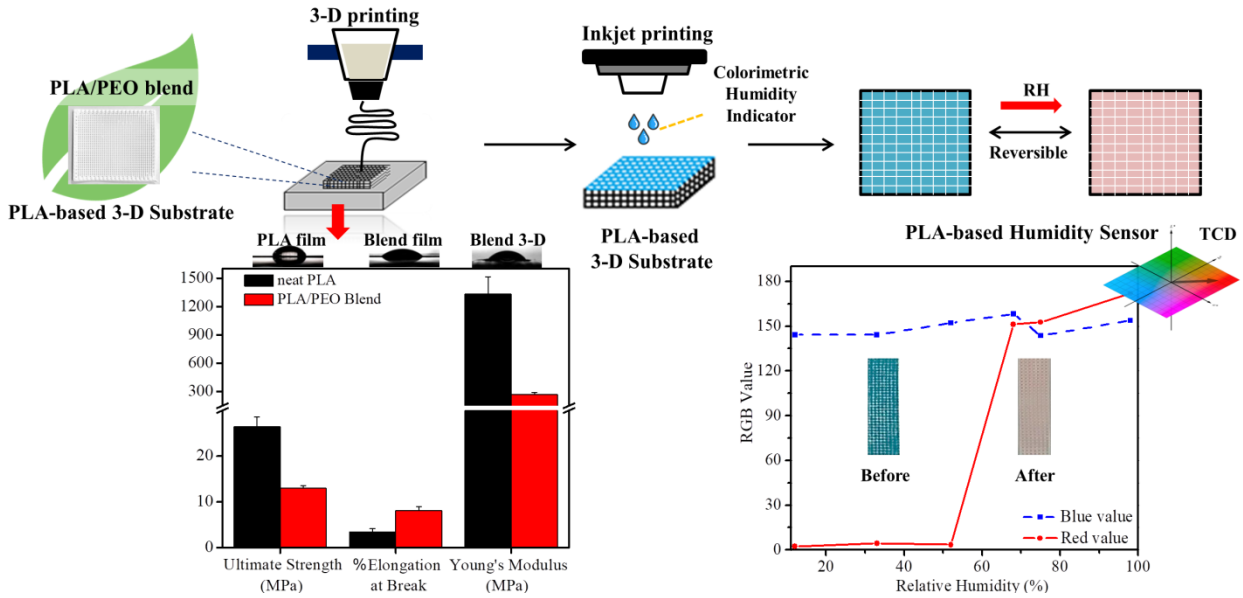

Abstract

This study aimed to fabricate biodegradable substrate with colorimetric humidity indicator for detective moisture in food packaging. The poor properties of poly(lactic acid) (PLA) were enhanced by melt blending PLA with non-toxic poly(ethylene oxide) PEO at 180 °C.

Specifically, three-dimensional (3D) substrates of PLA/PEO blends were fabricated by solvent-cast 3D printing. Furthermore, cobalt chloride ($CoCl_2$) solution was printed onto the substrate with an inkjet printer to serve as a colorimetric humidity sensing indicator. It found that the flexibility and thermal stability of the PLA were improved and the hydrophilicity was increased with an increase in PEO content. Color changes and the sensitivity of this material were confirmed using image analysis and total color difference. The $CoCl_2$ indicator displayed color changes that ranged from blue to pink under ambient conditions (above 60%RH), revealing suitable potential for frozen food packaging material with aim to detect amount of moisture in the packaging.

Keywords: Poly(lactic acid): Poly(ethylene oxide): Polymer blend: Colorimetric humidity sensor: 3D printing: Inkjet printing

1. Introduction

The development of biodegradable polymers for smart packaging to produce more environmentally friendly materials, such as poly(lactic acid) (PLA), has generated significant interest because of its biodegradability, non-toxicity, renewability, and compostability [Drumright, Gruber, & Henton, 2000]. PLA is a bioplastic that is derived from renewable agricultural resources and is being used in the food industry to package products or biomedical materials. However, the limitations of PLA and its applications are attributed to the brittleness of PLA as a substrate, as well as its poor thermal stability and hydrophobicity. Thus, its effective use in many applications has been limited [Auras, Harte, & Selke, 2004]. As a way of responding to the problems mentioned above, there has been greater interest and attention paid to mixing other biocompatible polymers with PLA by copolymerization [Phetsuk *et al*., 2020; Ruengdechawiwat *et al*., 2016] or blending [Suthapakti *et al*., 2017; Tuancharoensri, Ross, Mahasaranon, Topham, & S. Ross, 2017] in order to enhance the limitations of PLA.

Most research studies have blended polymers by way of solution blending methods that do not employ high-heat temperatures. This was done to avoid the degradation of polymers through the use of lower thermal degradation temperatures (T_d). Before the fabrication step, the melt-blending technique was performed to blend polymers without the need for solvents. This technique involved heating temperatures that were above the melting temperature of the polymers in order to achieve a homogeneous polymeric material [Arias, Heuzey, Huneault, Ausias, & Bendahou, 2014].

To improve the thermal properties, impact strength and hydrophilicity of PLA, it has been widely copolymerized or blended with various polymers to improve some of its advantageous properties. These polymers include natural rubber [Oyama, 2009; Ruengdechawiwat et al., 2016], poly(n-butyl acrylate) [Tachaphiboonsap & Jarukumjorn, 2003], poly(butylene succinate) [Lalita *et al*., 2013], polycaprolactone (PCL) [Hoidy, Al-Mulla, & Al-Janabi, 2010; Jompang *et al*., 2013], poly(ethylene glycol) (PEG) [Li, Liang, Zhang, & Zhu, 2015; Sheth, Kumar, Davé, Gross, & Mccarthy, 1997] or poly(ethylene oxide) (PEO) [Eom, Choi, & Park, 2019; Nijenhuis, Colstee, Grijpma, & Pennings, 1996; Oliveira *et al*., 2013; Saha, Samal, Biswal, Mohanty, & Nayak, 2018]. Several researchers have reported on the establishment of improved properties of

the PLA composites by adding PEG into the PLA matrix [Anderson & Hillmyer, 2004]. Remarkably, the addition of PEG content in PLA increased its ductility, thermal properties and mechanical properties [Li *et al*., 2015]. In addition, the biodegradation rate of PLA was also increased [Pasut *et al*., 2016]. The main function of PEG is as a polymeric plasticizer in the structure of the polymer chain [Gajria, Davé, Gross, & McCarthy, 1996]. According to Bailey et al., when the molecular weight of PEG exceeds 100,000 g/mol, it is named PEO [Bailey, Koleske, & Frederick, 1976]. PEO is a water soluble, nontoxic polymer with strong hydrophilic properties. Yoojun *et al*. focused on melt-blended PLA in different amounts of PEO and several researches also reported that the addition of PEO into PLA increased the flexibility, Izod impact strength and hydrophilicity of the PLA [Eom *et al*., 2019; Nijenhuis *et al*., 1996; Oliveira *et al*., 2013]. Through its effective application, humidity sensors using PEO electrospun fibre have been studied [Chen & Lu, 2005]. Under higher 87%RH, the opaque PEO electrospun fibre mesh became more transparent and began to fuse together. As mentioned above, PEO could be used for humidity monitoring with the naked eye, wherein low toxicity and irreversibility values can be determined. This opens up the opportunity to manipulate our environmentally friendly systems and use them as humidity sensors to demonstrate the broad applicability of this materials design approach.

Humidity sensors are a fast and reliable way of identifying when products have been exposed to a high humidity. Several different types of humidity sensors have been studied. Each of these sensors are based on a different principle. Some of the different sensors include capacitive, resistive, gravimetric and optical types [Gu, Huang, & Qin, 2004; Tian *et al*., 2008; Tsigara *et al*., 2007; Yu *et al*., 2006; Yu, Xy, Lee, & Li, 2013]. According to the relative humidity values (RH), humidity sensors can be classified into three types; a ceramic sensing material that uses porous materials to detect humidity, a semiconducting sensing material that uses a semiconductor and a polymer-based humidity sensor that uses semi-conductive properties to detect humidity. In previous research, polymer-based humidity sensors were investigated by measuring their response to humidity levels through changes in conductivity [Wang, Fu, Duan, & Li, 2015]. Two typical polyelectrolytes, poly(dimethyldiallylammonium chloride) and poly(sodium *p*-styrene sulfonate), were used for humidity detection. However, they are known to be non-biodegradable polymers. To easily detect humidity with the naked eye, color changes are observed in humidity sensors when several intermediate agents have been applied including photonic crystals [Hawkeye & Brett, 2011; Tian *et al*., 2008], polymer electrolyte thin films [Kim, Kim, Jo, Kim, & Park, 2012] and crystalline covalent organic framework nanofibers [Huang *et al*., 2013]. Furthermore, the most commonly known additives that are used as colorimetric humidity indicators, such as silica gel or cobalt(II) chloride [You *et al*., 2017], are currently being used in commercial applications. This work aimed to fabricate melt-blended PLA/PEO as the primary biodegradable substrate of humidity sensors and to coat a colorimetric humidity indicator onto the substrate by way of new printing technology. A humidity detector employing a polyester, such as PLA, will be fabricated. The detector will be safe for the environment because of its non-toxic biodegradable components.

In general, a simple technique of layer-by-layer (LbL) coating was used in the immersion (dip-coating) step when the substrate was immersed into the solution. However, this technique

commonly results in the production of chemical waste and is considered a time-consuming process that involves a series of dipping cycles [Akagi, Fujiwara, & Akashi, 2012]. With regard to current fabrication technology, three-dimensional (3D) and inkjet printing are now being widely used. These technologies offer several advantages when compared to other common methods. The advantages include the deposition of thin films that are considered both time-efficient and cost-effective because there is no need for an intermediate rinsing step [Akagi *et al*., 2012]. The process has also been easily automated as it involves high speeds and accomplishes room temperature deposition through easy control patterns and minimal thicknesses of the deposited material [Mensing, Wisitsoraat, Tuantranont, & Kerdcharoen, 2013]. In printed PLA studies, Guo and co-workers successfully fabricated the solvent-cast printing of a 3D microstructure from polylactide inks through the use of 3D printing [Guo, Heuzey, & Therriault, 2014]. The multifunctional microsystem of the PLA solutions by solvent-cast 3D printing was thoroughly investigated [Guo *et al*., 2013]. These novel 3D microstructure fabrications tend to use PLA solutions in various applications including tissue engineering scaffolds, stimuli-responsive materials and microelectronic devices [Guo *et al*., 2014]. However, these technologies have rarely been investigated with regard to the LbL fabrication of the colorimetric humidity indicator solution onto a polymer substrate.

In this work, a PLA biodegradable polymer blended with a non-toxic PEO polymer as environmental friendly materials to create a main humidity label substrate was investigated. A convenient, fast and various designs of 3D printing technique are interesting to design and control the PLA/PEO blends to fabricate a novel biodegradable substrate of humidity sensor for the first time. Moreover, a fast and continuous process of inkjet printing technique is interesting to coat $CoCl_2$ as a commercial colorimetric humidity indicator in a non-toxic amount to environmental and clearly seen a change in color. Therefore, PLA/PEO blends, the biodegradable and non-toxic materials can be fabricated to manipulate our environmental friendly system as an eco-friendly colorimetric humidity detective label.

2. Experimental

2.1 Raw materials

The poly(lactic acid) (PLA) resin used in this study was obtained from Bioplastic Production Laboratory for Medical Applications, Thailand, while the poly(ethylene oxide) (PEO) powder was purchased from Sigma-Aldrich, USA. The glass transition temperature (T_g) and melting temperature (T_m) of the PLA were 61 and 179°C, respectively. PEO with a weight-average molecular weight ($\bar{M}_w$) of 100,000-200,000 and a melting temperature (T_m) of 68°C was blended with PLA. Cobalt(II) chloride hexahydrate ($CoCl_2$•$6H_2O$) was obtained from QRëC, New Zealand. Chloroform ($CHCl_3$) and formic acid (≥98%) were purchased from Sigma-Aldrich, Germany. Dimethylformamide (DMF) (Fisher, England) was used as the solvent for $CoCl_2$•$6H_2O$ dissolution. All of the solvents were of analytical grade and were used without any further purification.

2.2 Preparation of PLA/PEO blends by melt-blending technique

The 3:1 PLA/PEO melt-blends were prepared from 5 %w/v polymer blends. The PLA pellets and PEO powder were mixed together before being melt-blended in an internal mixer (HAAKE™ Rheomix OS Lab Mixers). The mixtures were melt-blended for 8 minutes at 180 °C using a screw rotational speed of 130 rpm [Lalita et al., 2013]. A yellow homogenous compound was obtained and ground into pellets for use as feeding material in the 3D printing process.

2.3 3D Printing of PLA/PEO blends

Solvent-cast printing was performed to fabricate the 3D polymer substrate at ambient temperatures using a 3D printer (3D-bioplotter® EnivisionTEC). In order to study the 3D structure of the PLA/PEO blends for use as a substrate, a 3:1 ratio of the PLA/PEO blends obtained from the internal mixer was dissolved in the $CHCl_3$ solvent at concentrations of 20, 30 and 40 %w/v. Subsequently, various concentrations of the polymer solutions were allowed to rest in sealed bottom containers for 24 h at room temperature. After 24 h, the solutions were stirred and sonicated to obtain homogeneous polymer solutions before the 3D fabrication processing. Importantly, the viscosity of the polymer solution should be less than 1.0 dL/g. The polymer solutions were then loaded into a low-temperature cartridge at 25 °C.

The applied pressure and printing speeds were within the range of 3-4.5 bars and 25-30 mm/s, respectively, while all gauge sizes were also studied. The "VisualMachine" computer program was used to control the printing process and "Solid works" was used to design a layer-by-layer 3D structure to determine the desired size, shape and thickness.

2.4 Fabrication of colorimetric humidity sensors by inkjet printing

Cobalt chloride solution was used as the ink for inkjet printing. The ink was prepared by dissolved $CoCl_2 \cdot 6H_2O$ in dimethylformamide (DMF) and was filtered (through a pore size of less than 0.30 μm) and loaded into a cartridge before the fabrication process. A commercial inkjet material printer, Fujifilm Dimatrix DMP 2800 piezoelectric inkjet printer, was used to print the ink onto the 3D substrate without an intermediate rinsing step. The "Drop Manager" computer program was used to control the printing process with 20 jetting nozzles and 32V firing voltage. The printing process was repeated by applying 4 cycles of the ink on the 3D substrate over a square-shaped area of 4 cm × 4 cm. The processing time per cycle was about 180 s.

2.5 Measurements

2.5.1 PLA-based substrate improvement

Fourier transform infrared (FTIR) spectroscopic analysis was performed with a wavenumber range between 600-3200 cm^{-1}. Differential scanning calorimeter (DSC, Perkin-Elmer DSC7) was used to determine the thermal properties of the various substrates with a heating rate of 10 °C/min from 0 to 220 °C. The weight loss value and degradation temperature were determined using thermogravimetric analysis (TGA, Perkin-Elmer TGA7) at 20 °C/min from 50 to 550 °C in a nitrogen atmosphere. Tensile tests were performed using a universal testing machine (Lloyds LRX+ Universal Mechanical Testing Machine) to determine the tensile strength and elongation at break with a loading cell of 10 N. The tensile speed was 10 mm/min

and a 50 mm gauge length was used. A dimension of each test specimen was 70 mm × 10 mm (length × width) with a thickness of ~0.1 mm. All samples were tested 5 times and the average values were reported. The surface morphology was observed using a scanning electron microscope (SEM, JEOL 5910 LV), while energy dispersive x-ray analysis (EDX, JEOL 5910 LV) was used to identify the elemental composition on the substrate. The degree of surface wettability was then evaluated by water contact angle measurement.

2.5.2 PLA-based humidity sensor for color observation

To determine humidity measurements, saturated salt solutions were used in closed containers that contained saturated lithium chloride (~12% RH), saturated magnesium chloride (~33% RH), saturated magnesium nitrate (~52% RH), saturated copper(II) chloride (~68), saturated sodium chloride (~75%RH) and water (~100% RH) in order to establish humidity control. To observe changes in colors, photographs of the samples were taken with a digital camera (Canon EOS1100D). The RGB of the images [Bridgeman, Corral, Quach, Xian, & Forzani, 2014] were analyzed with the use of the "Photoshop" computer program. Colorimeter (MINOLTA CR-400) was then used to determine the total color difference (TCD) using the following equation [Díaz, Candia, & Cobos, 2016; Díaz, Ferreiro, Rodríguez-Otero, & Cobos, 2019]:

$$TCD = [(\Delta L^*)^2 + (\Delta a^*)^2 + (\Delta b^*)^2]^{1/2} \qquad \text{Eq. (1)}$$

where ΔL^*, Δa^* and Δb^* are representative of the differentials of lightness, green and yellow between the samples and the initial labels, respectively.

3. Results and discussion

3.1 Property improvement of PLA/PEO blends

3.1.1 FTIR spectroscopy

Among various spectroscopic techniques, FTIR spectroscopy is commonly used in analyzing the interaction between PLA and PEO. Both spectral band width and intensity may be correlated with the strength and extent of hydrogen bonding [Oliveira *et al*., 2013]. Two completely incompatible polymers show no spectral interaction, whereas compatible polymers that do have chemical interactions reflect such changes in the IR spectrum in the form of band shifts, band widening and changes in band intensity [Oliveira *et al*., 2013].

The IR spectra (600–3200 cm^{-1}region) of the PLA/PEO mixtures were consistent with chemical interactions between PLA and PEO (Figure 1). In the spectrum of the 3:1 PLA/PEO blend, all the featured FTIR absorption peaks of PLA and PEO were almost similar. This would indicate the non-existence of any chemical interactions within the blended films. Additionally, no new bands were formed or strong chemical interactions occurred with the polymer blends. From Table 1, a decrease in C—O—C (carbonyl) stretching can be seen in regards to the CH_3 stretching vibration for the 3:1 PLA/PEO blend in comparison with PLA. This was determined to be a consequence of the redistribution of the helical structure of PLA. This revealed that the α crystal structure of the PLA has been partially converted into the β crystal structure due to a

change in its helical conformation during crystallization, thus indicating the effect of PEO as a β nucleating agent [Saha *et al*., 2018].

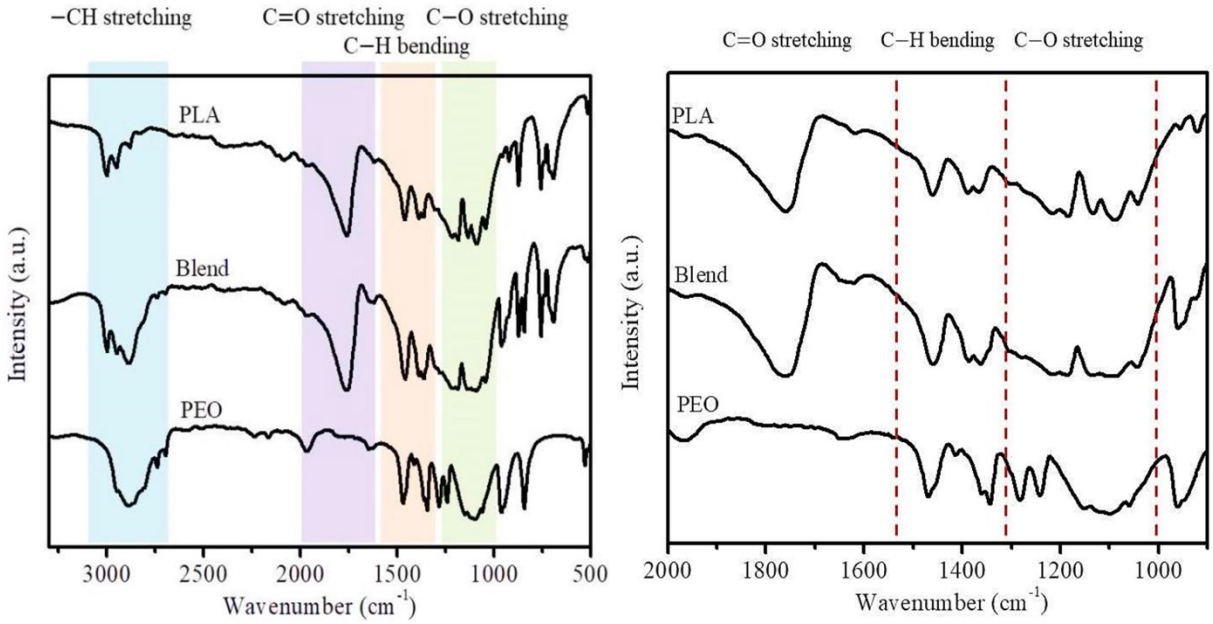

Figure 1. FTIR spectra of neat PLA, 3:1 PLA/PEO blend and neat PEO (left) and focus in 900-2000 cm^{-1} range (right).

Table 1. FTIR ratio of the neat PLA, 3:1 PLA/PEO blend and the neat PEO.

Assignment	Wavenumber (cm^{-1})	FTIR ratio		
		Neat PLA	3:1 PLA/PEO blend	Neat PEO
COC/CH_3	1087/1460	0.8	0.3	-
C=O/CO	1760/1107	-	0.9	-

3.1.2 Thermal properties tests

The DSC thermogram was carried out to analyze the thermal properties *via* the second heating run. The thermal properties included the glass transition temperature (T_g), crystallization temperature (T_c), melting temperature (T_m), and the decomposition temperatures (T_d) which are all presented in Table 2. The T_m of the neat PLA and PEO values were 178.8 and 67.7 °C, respectively and indicated that polymers are the semicrystalline. The T_m of the PLA/PEO blends derived from both PLA and PEO were recorded at 171.7 and 54.2 °C, respectively. The results indicated compatibility of the PLA/PEO blends when the blends are mixed using an internal mixer. Blending PLA with PEO also slightly reduced the T_g, T_c and T_m values when compared with PLA. Similar results were reported by Sara et al. and Yoojun et al. also found that the addition of PEO content into PLA decreased the T_g, T_c, and T_m values [Eom et al., 2019; Oliveira *et al*., 2013; Saha *et al*., 2018]. A decrease in T_g indicated that PEO could enhance the chain mobility of PLA. Moreover, a decrease in the T_c value from 120.5 °C to 115.0 °C, when PEO was added into the PLA, indicated that PLA crystallized at lower temperatures. This was due to the

fact that PEO accelerated the crystallinity of the blends. In addition, PEO was found to be good for the mobility of the molecular chain due to a plasticizing effect of PEO on the PLA matrix [Eom *et al*., 2019; Li, Zhang, Liang, & Wang, 2015; Park, Song, Park, & Yoon, 2011]. Furthermore, it was deemed beneficial as it increased its flexibility which is desirable when it is used as a substrate.

In order to investigate thermal stability, thermalgravimetric analysis was performed on the neat PLA, neat PEO and the 3:1 PLA/PEO blend. The thermal degradation behavior of the relative weight loss as a function of temperature was determined from the thermalgravimetric curves. The TGA thermograms exhibited important weight loss over the temperature range. An increase in the T_d value of the PLA/PEO blends indicated that the temperature at 95% weight loss increased from 390.6 (neat PLA) to 405.2 (3:1 PLA/PEO blends). Furthermore, the temperature increased to 435.8 °C when compared to that of the neat PEO. Moreover, in agreement with Yoojun *et al*., the addition of PEO content in PLA gradually increased the thermal stability of the PLA [Eom *et al*., 2019]. The main thermal characteristic data of the neat PLA, neat PEO and the 3:1 PLA/PEO blends are presented in Table 2. Remarkably, the 3:1 PLA/PEO blends displayed better thermal stability than the neat PLA.

Table 2. Thermal properties of PLA, PEO and PLA/PEO blend.

	T_g (°C)	T_m (°C)	T_c (°C)	T_d (°C)	ΔH_{cc} (J/g)	ΔH_m (J/g)
Neat PLA	60.8	178.8	120.5	390.6	32.7	45.0
PLA/PEO blend	54.8	171.7	115.0	405.2	35.5	40.6
Neat PEO	-	67.7	-	435.8	-	103.3

3.1.3 Mechanical properties test

The mechanical properties of the neat PLA and 3:1 PLA/PEO blended films, such as tensile strength (MPa) and elongation at the break (%), were studied and the results are presented in Table 3 and Figure 2. Figure 2 displays comparisons of the mechanical properties between neat PLA and PLA/PEO blends. Ultimate strength and elongation values at the break of neat PLA film, as shown in Figure 2(a), were 26.4 MPa and 3.4%, respectively. The ultimate strength, modulus and elongation at break of the 3:1 of PLA/PEO blended film moderately decreased from 26.4 to 13.0 MPa, 1333.0 to 266.4 MPa and increased from 3.4 to 8.1%, respectively when compared with the neat PLA film. The results indicate a decrease in ultimate strength and modulus of the neat PLA film along with the addition of PEO content, whereas the elongation at break of the PLA/PEO blended film increased by twice as much as the neat PLA film. A significant decrease in the ultimate strength and modulus, as well as a two-fold increase in the elongation at the break, was caused by PLA plasticizing with PEO. Similar studies on the mechanical properties of the PLA and PLA/PEO blended films have been reported [Eom *et al*., 2019; Nijenhuis *et al*., 1996; Saha *et al*., 2018]. It has been further reported that the addition of 5 wt% PEO in the PLA caused a decrease in the ultimate strength of the PLA/PEO blended film, while the elongation at the break increased due to the plasticizing effect of PEO [Nijenhuis *et al*., 1996]. Sara et al. reported that by adding PEO content by over 4 wt%, a sharp decrease in tensile strength occurred. This outcome is related to the phase separation of PEO over 4 wt% in the PLA

matrix. In addition, a decrease in tensile strength and an increase in elongation at break are consequences of the increasingly rubbery nature of PLA when it is mixed with PEO. Therefore, the presence of PEO content could improve the mechanical properties of PLA as a result of the plasticizer property within the structure of PEO.

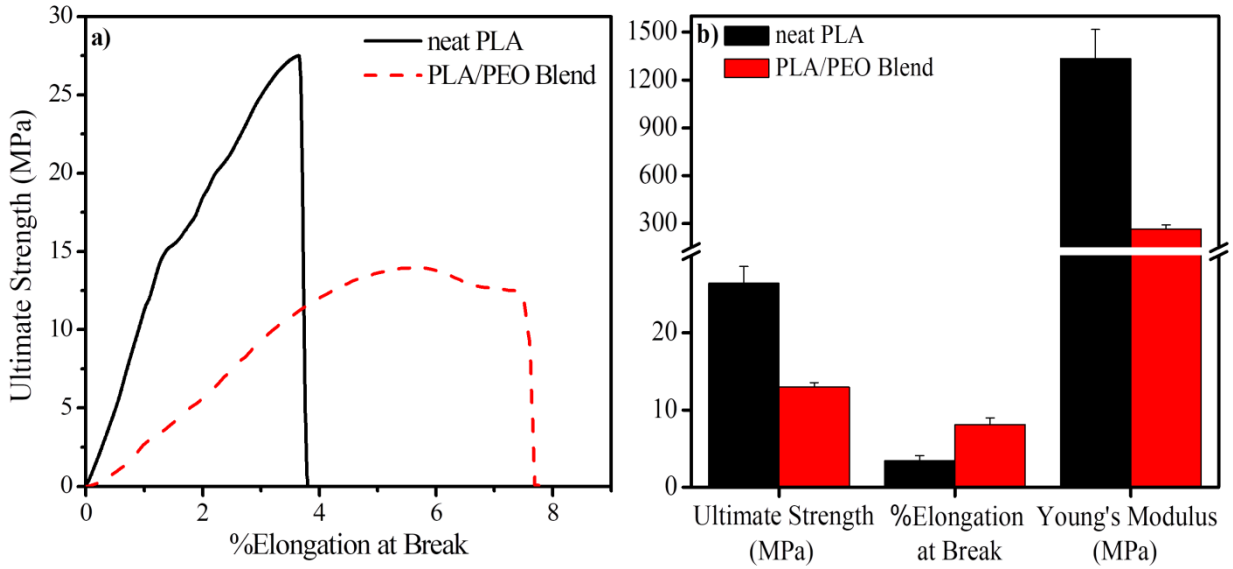

Figure 2. Mechanical properties of neat PLA film and 3:1 PLA/PEO blended film: (a) Stress-strain curves and (b) Mechanical properties comparison.

Table 3. Tensile properties of PLA and PLA/PEO blended films.

Sample	Ultimate Strength (MPa)	Elongation at break (%)	Young's modulus (MPa)
Neat PLA film	26.4 ± 2.2	3.4	1333.0 ± 184.4
Polymer blends film	13.0 ± 0.7	8.1	266.4 ± 25.2

3.1.4 Water contact angle

A suitable substrate should easily absorb water for the surface coating process. To compare the surface wettability of various substrates, the water contact angle is used to indicate the hydrophilicity of the substrate. As is evident from Table 4, the water contact angle of the neat PLA film and the 3:1 PLA/PEO blended film were 71.19° and 48.07°, respectively. When PEO content was added to the PLA, the water contact angle decreased due to an increase in the hydroxyl groups (-OH) of PEO in the PLA structure. In nature, PEO is more hydrophilic and is a polymeric amphiphile that contains a nonpolar hydrophobic region (ethylene unit) and a polar hydrophilic region (ether oxygen) in the polymer chain [Bailey *et al*., 1976]. Moreover, the plasticizing effect of PEO encouraged the diffusion of water molecules through chain mobility [Nijenhuis *et al*., 1996]. A similar study conducted by Juliano *et al*. determined that the contact angle for various PEO concentrations added to the PLA indicated that the contact angle for all the blended samples (1:0, 1:3, 1:1, 3:1, and 0:1 PLA/PEO ratios) was within the ranges of the neat PLA (120°) and the neat PEO (38°).

Furthermore, no significant differences were observed between the 3:1 PLA/PEO blended film and the 3D substrate of 3:1 PLA/PEO blends. The smooth surface of the blended films resulted in lower contact angles compared to the rough surface of the 3D blended substrate. The 3:1 PLA/PEO blend had the lowest contact angle and the results indicate that some of the PEO was exposed on the surface in each of the blends. When the surface came in contact with a water droplet, the PEO fraction on the surface absorbed the water droplet. As a result, PEO enhances the hydrophilicity of PLA and this is useful in the process of coating the substrate.

Table 4. Water contact angle analysis of neat PLA film, 3:1 PLA/PEO blended film and 3D substrate of PLA/PEO blend.

Sample	Water contact angle (°)	
Neat PLA film		71.2 ± 0.4
Polymer blends film		48.1 ± 2.4
3D of Polymer blends	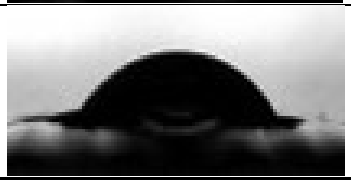	55.7 ± 0.6

3.1.5 Surface morphology

The surface morphology of various substrates was studied with the use of a scanning electron microscope (SEM) and a light microscope. The SEM images of the neat PLA film, the polymer blended film and the 3D substrate of the polymer blends are shown in Figure 3. For the surface analysis, the neat PLA film (Figure 3(a)) had a smooth surface and was not found to be porous. Thus, it displayed poor ability to hold and absorb both water and ink. While adding PEO content to PLA, the substrate of the 3:1 ratio of the PLA/PEO blended film (Figure 3(b)) was more porous and the unequal size of the pores allowed water or ink to spread throughout the film. This porous microstructure of the 3:1 PLA/PEO blended substrate resulted in an inferior barrier property, forming diffusion pathways for oxygen and water vapor [Saha *et al*., 2018]. Consequently, the water absorption of the polymer blended film was found to be better than the neat PLA film due to its porous surface and the hydroxyl groups of the PEO structure. Figures 3(c)-(d) present microscopic images that clearly show the substrate coated with $CoCl_2$ were blue, while prior to coating the substrate appears to be white. This occurs because of the presence of a larger number of cavities and thus surface area. This was due to both the design and the fabrication technique that was used. Thus, the substrate was able to absorb both water and ink, which ultimately increased the number of opportunities for interactions with its surroundings.

Post coating the surface with $CoCl_2$ solution by inkjet printing, EDX was used to identify the elemental composition on the surface. EDX spectrums are displayed as insets in Figures 3(e)-(f). The elements on the surface included Co, Cl, O and C, as shown in Table 5. Therefore, the EDX results confirmed that the 3D substrate of the 3:1 blend of PLA/PEO could be successfully coated with cobalt chloride solution with the use of inkjet printing technology.

In this research, the PLA biodegradable polymer was blended with biodegradable counterparts, such as PEO non-toxic polymers, to develop a safe substrate for environmentally friendly materials and to also retain the biodegradability of PLA. Moreover, the $CoCl_2$ solution as a humidity indicator coated the 3D substrate via inkjet printing technology in small picolitres in order to be conscious of certain potential environmental problems.

According to findings of the previous studies mentioned above, the 3:1 PLA/PEO blend has optimal ratios of PLA and PEO blending for use in fabricating a 3D substrate of colorimetric humidity sensors. With regards to the thermal properties, DSC confirmed that the plasticizing effect of PEO enhances chain mobility of PLA, while TGA confirmed the addition of PEO increased the thermal stability of PLA. Moreover, the surface wettability and flexibility of PLA were improved by blending PLA with PEO. According to surface morphology, the film surface of the 3:1 PLA/PEO blend was more porous, which resulted in the creation of easier diffusion pathways for oxygen and water vapor. A similar finding has also been observed in a study involving three mixtures of PLA/PEO blends (3:1, 1:1 and 1:3). A 3:1 ratio of the solution blend of PLA/PEO was found to be the most homogenous and best in terms of its miscibility [Oliveira *et al*., 2013].

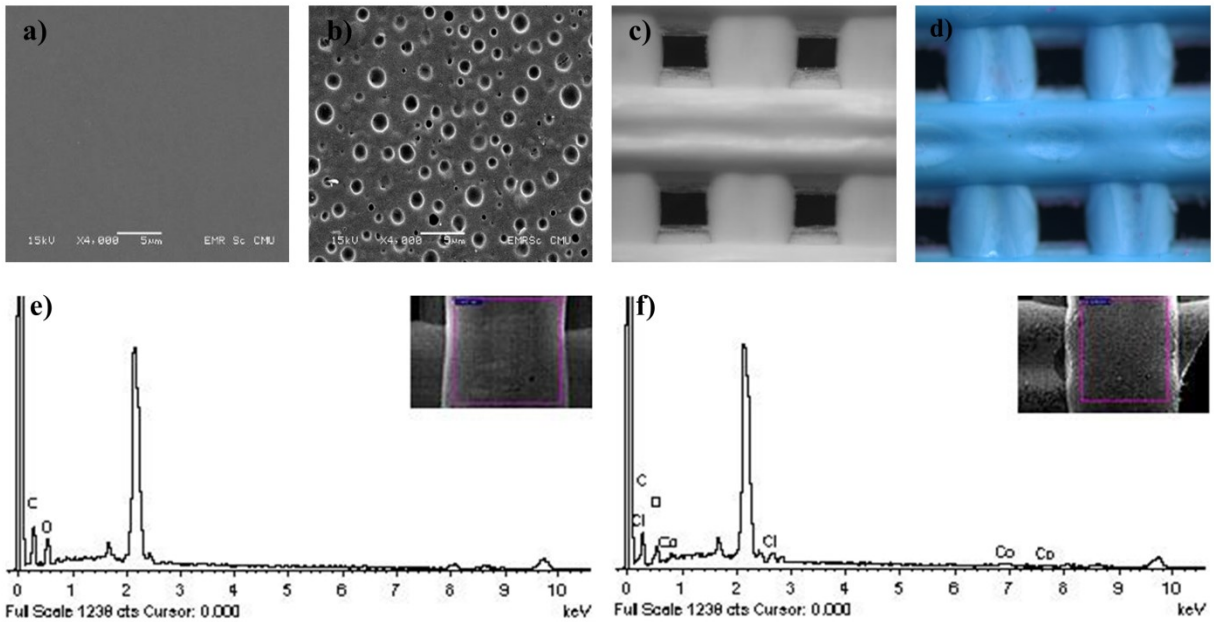

Figure 3. SEM images, (a) neat PLA film (×4000); (b) 3:1 PLA/PEO blended film (×4000), Microscopic images, (c) 3D substrate of 3:1 PLA/PEO blend (×200); (d) 3D substrate coated with $CoCl_2$ and EDX analysis (e) uncoated 3D substrate and (f) 3D substrate coated with $CoCl_2$.

Table 5. Chemical composition on the surface of polymer blended 3D substrate.

Sample	Chemical composition (% Weight)			
	C	O	Co	Cl
Uncoated	48.85	51.15	-	-
Coated by 4 layers of $CoCl_2$	55.99	26.27	6.52	11.22

3.2 Color observation

3.2.1 Colorimetric humidity sensors through printing technology

In accordance with the positive points mentioned above, the 3:1 PLA/PEO blend was also fabricated as a solvent-cast by 3D printing to establish a 3D substrate. The 3D substrate was designed in spherical and square shapes, as shown in Figure 4(a). The main parameters in this work included applied pressure, printing speed, nozzle diameter (Gauge size) and a concentration of the 3:1 PLA/PEO blended solution. The suitable applied pressure and printing speed were within the range of 3-4.5 bars and 25-30 mm/s, respectively. The studied concentrations of the polymer solution were 20, 30 and 40 %w/v. To fabricate a 3D structure, a smaller nozzle diameter is required for faster solvent evaporation and a higher degree of viscosity of the solution. High concentrations of the solutions, increased printing speeds, reduced nozzle diameter or a reduction in the applied pressure enabled faster solvent evaporation rates to rapidly enhance the rigidity of the 3D structure in order for it to support itself after extrusion [Guo *et al*., 2014]. Thus, the solvent evaporation rate and viscosity of the solution must be suitable for effective fabrication. In addition, adequate viscosity of the solution is required to allow oxygen and water vapor to flow easily through the nozzle and to achieve a smooth filament [Guo *et al*., 2014]. A 40 %w/v solution was not effectively fabricated because it was not able to flow smoothly through the nozzle with a degree of high viscosity. A 20 %w/v solution was unable to flow continuously through the nozzle as the viscosity was too low and it did not exhibit enough rigidity to support itself after extrusion [Guo *et al*., 2013; Guo *et al.*, 2014]. Notably, the 30 %w/v of 3:1 PLA/PEO blend solution successfully fabricated the 3D substrate. Four layers at a thickness of ~ 0.3 mm, with square-shaped areas of 5 cm × 5 cm and spherical shapes that were 5 cm in diameter of the 3D substrates were fabricated before being coated with the $CoCl_2$ solution by inkjet printing.

The $CoCl_2$ solution that was used as ink was successfully prepared by dissolving 50 wt% of $CoCl_2$ in DMF solvent and then printed by inkjet onto the 3D substrate of the 3:1 PLA/PEO blends. The solution had particles that were below 0.30 µm pore size of the fluids using a 0.30 µm syringe filter. The 4×4 cm square-shaped areas of the $CoCl_2$ solution with the four-layered materials were printed on the 3D substrates, EDX spectrum confirmed that the relevant elements, including Co, Cl, O and C, were coated onto the surface of the 3D substrate.

3.2.2 RGB analysis

For the detection of humidity, the RGB value was used to confirm the color changes [Bridgeman, Corral, Quach, Xian, Forzani, 2014; Hirayama, Takayama, Haruta, Ishibashi, Takeuchi, 2017] of the colorimetric humidity sensors via “Adobe Photoshop”. With higher levels of humidity, the photographs of the samples appeared to become more concentrated as the color

changed from pink from blue. The red and blue value changes of the samples at various relative humidity levels (12-100 %RH) indicated that the colorimetric humidity sensors could be used to determine the presence of moisture in the surrounding environment. Above 60%RH, the red value was significantly increased along with an increase in relative humidity from 3.5 to 151.2 at 68%RH, as is shown in Figure 4(b)-(c). As can be seen in the photographs, when these colorimetric humidity sensors were exposed to relative levels of humidity, the color changed from blue at low relative humidity levels (12-60 %RH) to pink at high relative humidity levels (above 60%RH). Remarkably, the RGB results corresponded to the photographs of the samples when exposed to different humidity levels.

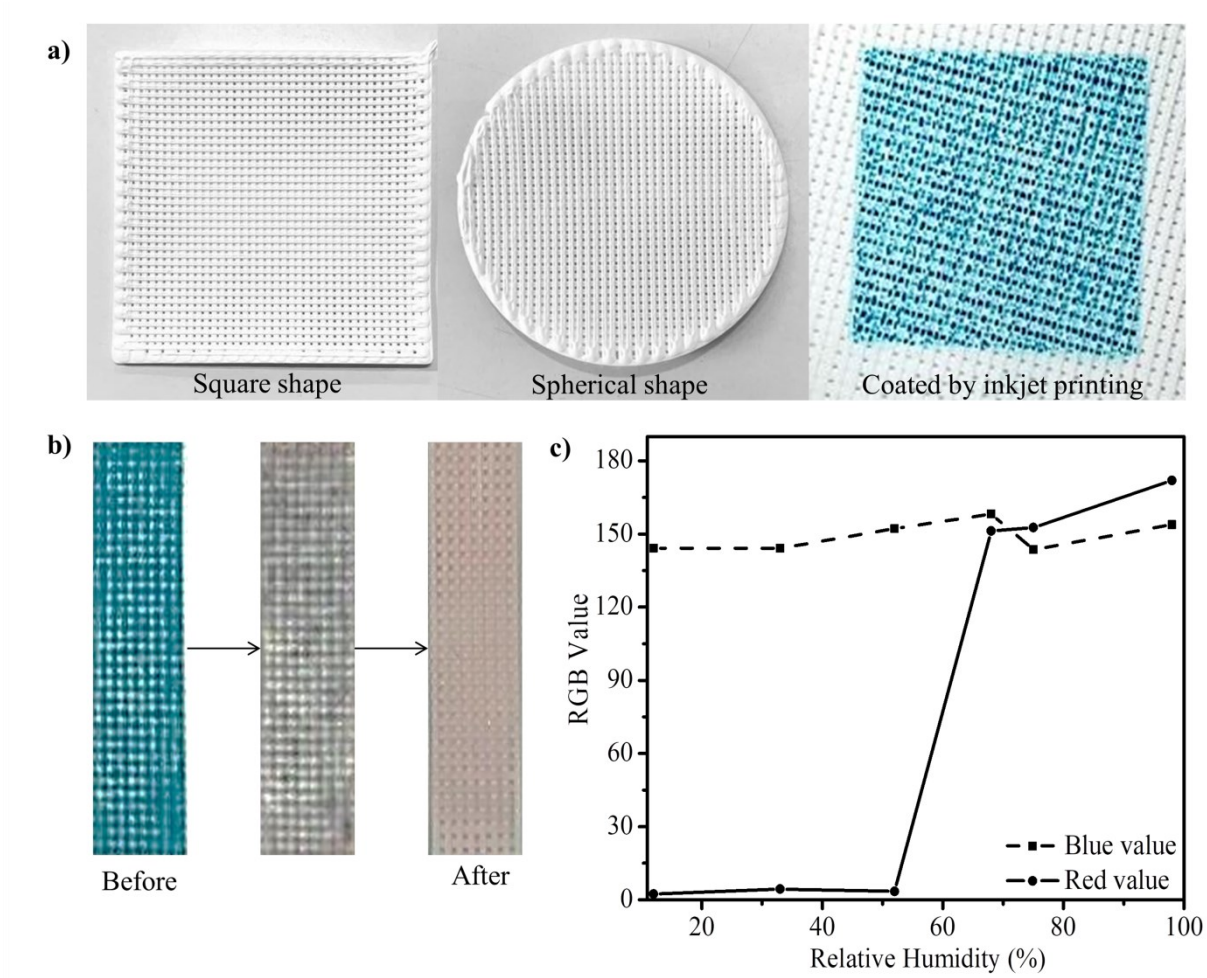

Figure 4. Materials color observation; a) Photographs of 3D substrates in square-shape, cylindrical-shape and coated with the $CoCl_2$ solution applied by inkjet printing, respectively; b) photograph of color changes during the test of the sensors (blue to pink); c) RGB analysis of photographs of colorimetric humidity sensors when exposed to different levels of humidity.

As is evident in Figure 4(b), this reaction is a hydration reaction with $CoCl_2$ absorbing water. As the humidity increases two water molecules surround each cobalt atom. Subsequently, cobalt chloride dihydrate is formed as shown in equation (2) and the color purple is observed. As the humidity increases further, the crystal structure of the cobalt chloride rearranges itself to

allow four more water molecules to surround each cobalt atom. The cobalt chloride hexahydrate is subsequently formed as shown in equation (3) and a pink color observed [Tsigara *et al*., 2017, You *et al*., 2017].

$$CoCl_2 + 2H_2O \rightarrow CoCl_2 \cdot 2H_2O\ (Dihydrate) \qquad \text{Eq. (2)}$$

$$CoCl_2 \cdot 2H_2O + 4H_2O \rightarrow CoCl_2 \cdot 6H_2O\ (Hexahydrate) \qquad \text{Eq. (3)}$$

3.2.3 Repeatability

The response and recovery behavior of the colorimetric humidity sensors are important properties for the accuracy of these sensors. The time taken for the color changes were tested by alternating the sensors between closed containers at either high humidity levels (68-96% RH) or low humidity levels (21% RH), respectively for 5 cycles. This was carried out for 3 conditions which correspond to 21-68% RH, 21-75% RH and 21-96% RH. The dip-coated polymer blended films with 50% $CoCl_2$ solution, dipped for various times (1, 3, and 5 minutes), were compared with the 3D coated polymer blend with the 50% $CoCl_2$ solution applied by inkjet printing. Figure 5 presents the response and recovery times of the colorimetric humidity sensors that were used to evaluate the accuracy of these sensors [You *et al*., 2017]. The results of these three conditions indicate that the response time of each sample was influenced by the humidity conditions, while each cycle displayed a similar saw-tooth shape. For humidity sensing, the PLA/PEO blended substrates coated with 50% $CoCl_2$ exhibited good repeatability behavior at different humidity levels. Furthermore, the sensitivity of these sensors differed after different coating techniques were used, wherein the four-layer inkjet-coating sensors at the highest humidity level yielded overall color changes of less than 50 minutes (black solid line) when compared to the dip-coated sensors. On the other hand, the sensitivity of the inkjet-coated sensors was higher or similar to that of the dip-coating sensors at 96%RH (highest humidity). This would suggest that the amount of the colorimetric sensing solution affects the sensitivity of the sensors in accordance with a small (picolitre) drop volume of the inkjet coating method.

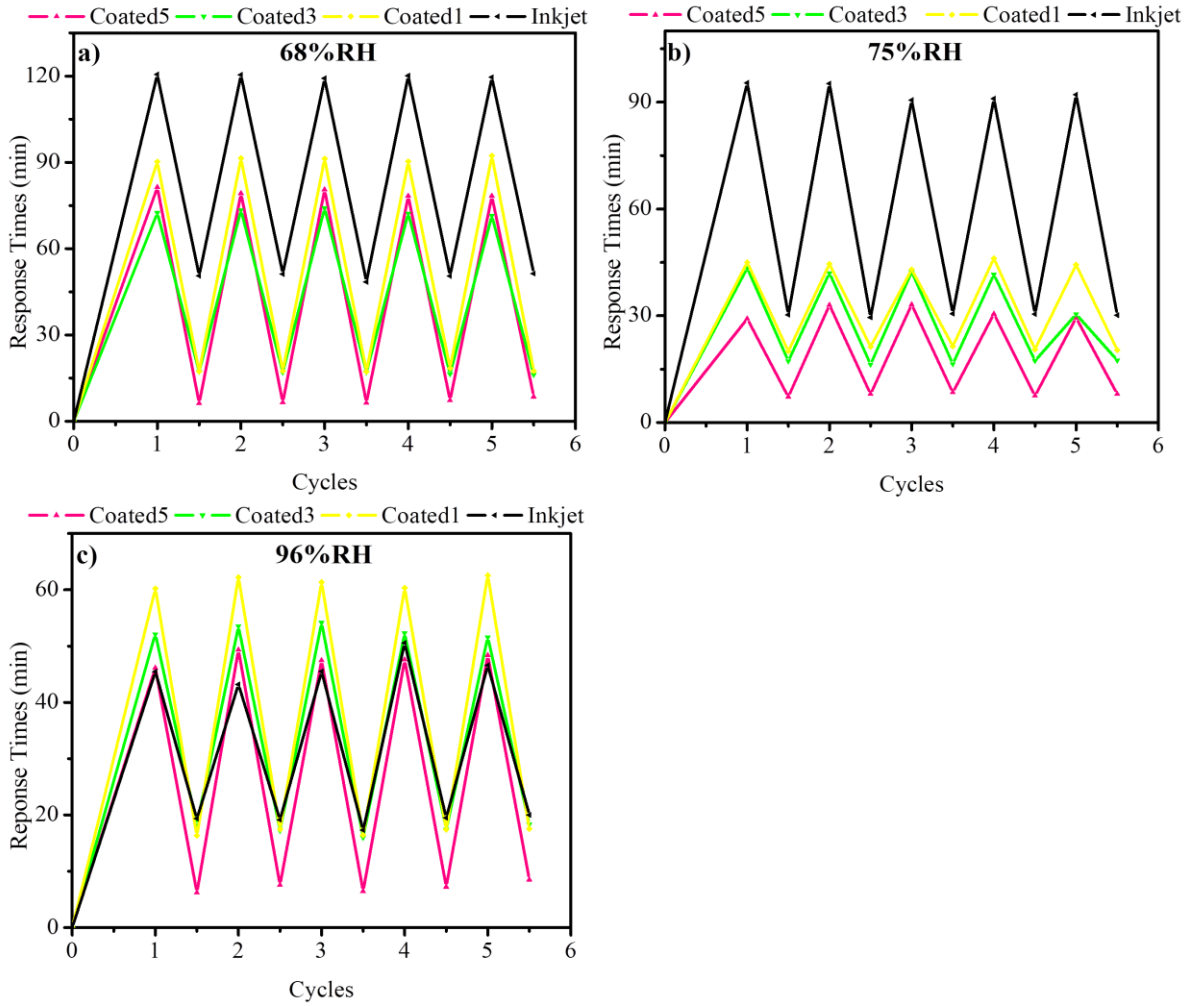

Figure 5. RGB analysis of photographs of colorimetric humidity sensors when exposed to different humidity levels: a) 68% RH; b) 75% RH; c) 96% RH.

3.2.4 Total color difference (TCD)

Total color difference (TCD) was studied to determine the sensitivity of the color changes of the colorimetric humidity sensors at different times. The samples obtained under different humidity levels were indicated by lightness (L^*), green color (a^*), yellow color (b^*) and total color difference (ΔE) between the final and initial labels, respectively [Díaz et al., 2016; Díaz et al., 2019]. Furthermore, %RH significantly affected the color changes at various times. At 96%RH, the humidity sensors appeared to become gradually brighter with time (L^*>0), redder (a^* >0) and less blue (b^* >0). Color changes of the $CoCl_2$ humidity indicator were observed at the a^* and b^* values. As is evident from Table 6 and Figure 6, a^*, b^* and ΔE tended to increase over time as compared to the initial color of the humidity sensors at 96 %RH (the highest %RH value). These results are consistent with the RGB results. As the sensitivity at the highest %RH of these sensors, TCD initiated an increase within 5 minutes and clearly changed color at 40 minutes.

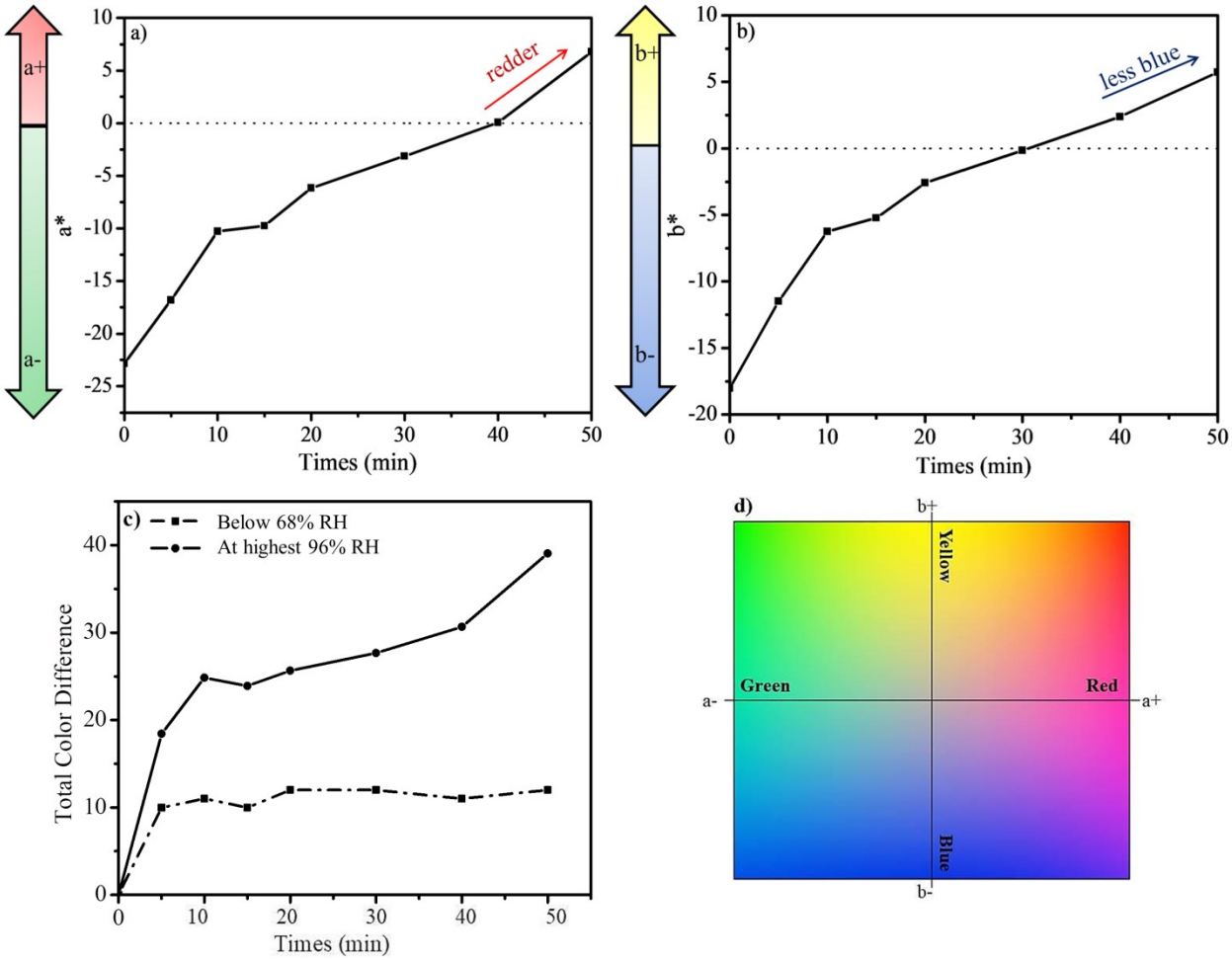

Figure 6. TCD for color change of the colorimetric humidity sensors at different times; a) a*; b) b* at highest 96%RH; c) ΔE of the color change and d) CIELAB color chart.

Table 6. Total color difference of colorimetric humidity sensors at the highest %RH (96%).

Time (min)	*L**	*a**	*b**	Δ*E*
0 Initial sample (Blue color)	74.81	-22.82	-18.03	0
5	68.66	-16.80	-11.50	10.80
10	56.91	-10.29	-6.24	24.83
15	59.42	-9.77	-5.24	23.90
20	62.85	-6.17	-2.60	25.66
30	67.21	-3.13	-0.17	27.65
40	75.26	0.06	2.38	30.66
50 Final sample (Pink color)	84.15	6.77	5.70	39.06

4. Conclusions

To enhance the poor thermal properties of PLA, along with its low flexibility and poor hydrophilicity, a preparation of PLA was successfully melt-blended at 180 °C for 8 minutes with PEO at a ratio of 3:1 PLA/PEO. The flexibility of the PLA/PEO blend increased with the addition of PEO. The hydrophilicity of the 3:1 PLA/PEO blend and the thermal stability of PLA were

found to be enhanced when compared with neat PLA. The morphology of the polymer blends indicated the establishment of good substrate properties. This was the result of a more porous structure spread throughout the surface which resulted in inferior barrier properties. A 30 %w/v of the PLA/PEO blend solution in chloroform solvent was used to fabricate the 3D substrate by 3D printing. This approach was then used to create a custom-made environmentally friendly colorimetric humidity sensor. For the coating step, inkjet printing technology was used to coat a $CoCl_2$ solution onto the 3D polymer substrate with the use of a commercial inkjet material printer. The optimal ink for the colorimetric humidity indicator was prepared from 50 %w/v $CoCl_2$ in the DMF solvent. The colorimetric humidity sensors clearly exhibited different colors within 40 minutes over the range of 60-100 %RH. This outcome indicated that the 3D substrate coated with $CoCl_2$ has promising potential for applications in product humidity monitoring. Moreover, the advantages of this technology, such as high-frequency continuous operation, small volumes and highly controlled ink-drop patterning, can be applied to other polymers for alternative novel innovations using environmentally friendly materials.

5. Acknowledgements

This research was financially supported by the Program Management Unit for Human Resources & Institutional Development, Research and Innovation, Office of National Higher Education Science Research and Innovation Policy Council (NXPO) [Grant Number B16F640001]; National Electronics, Computer Technology Center (NECTEC), National Science and Technology Development Agency (NSTDA); the Center for Innovation in Chemistry (PERCH-CIC) and the Center of Excellence in Materials Science and Technology, Chiang Mai University. This project also received funding from the European Union's Horizon 2020 research and innovation programme under Marie Sklodowska-Curie grant agreement No. 871650 (MEDIPOL).

References

Akagi, T., Fujiwara, T., Akashi, M. (2012). Rapid Fabrication of Polylactide Stereocomplex Using Layer-by-Layer Deposition by Inkjet Printing, Angewandte Chemie International Edition, 124(22), 1-5.

Anderson, K.S. & Hillmyer, M.A. (2004). The Influence of Block Copolymer Microstructure on the Toughness of Compatibilized Polylactide/Polyethylene Blends, Polymer, 45(26), 8809-8823.

Arias, A., Heuzey, M.C., Huneault, M.A., Ausias, G., & Bendahou, A. (2014). Enhanced Dispersion of Cellulose Nanocrystals in Melt-Processed Polylactide-Based Nanocomposites, Cellulose, 22(1), 483-498.

Auras, R., Harte,B., & Selke, S. (2004). An Overview of Polylactides as Packaging Materials, Macromolecular Bioscience, 4(9), 835-864.

Bailey, F.E., Koleske, J.V., & Frederick, E. (1976). Poly(ethylene oxide). Academic Press, Cambridge.

Bridgeman, D., Corral, J., Quach, A., Xian, X., & Forzani, E. (2014). Colorimetric Humidity Sensor Based on Liquid Composite Materials for the Monitoring of Food and Pharmaceuticals, Langmuir, 30(35), 10785-10791.

Chen, Z. & Lu, C. (2005). Humidity Sensors: A Review of Materials and Mechanisms, Sensor Letters, 3(4), 274-295.

Díaz, O., Candia, D., & Cobos, Á. (2016). Effects of Ultraviolet Radiation on Properties of Films from Whey Protein Concentrate Treated Before or After Film Formation, Food Hydrocolloids, 55, 189-199.

Díaz, O., Ferreiro, T., Rodríguez-Otero, J., & Cobos, Á. (2019). Characterization of Chickpea (Cicer arietinum L.) Flour Films: Effects of pH and Plasticizer Concentration, International Journal of Molecular Sciences, 20(5), 1246-1261.

Drumright, R.E., Gruber, P.R., & Henton, D.E. (2000). Polylactic Acid Technology, Advanced Materials, 12(23), 1841-1846.

Eom, Y., Choi, B., & Park, S. (2019). A Study on Mechanical and Thermal Properties of PLA/PEO Blends, Journal of Polymers and the Environment, 27(2), 256-262.

Gajria, A.M., Davé, V., Gross, R.A., & McCarthy, S.P. (1996). Miscibility and Biodegradability of Blends of Poly(lactic acid) and Poly(vinyl acetate), Polymer, 37(3), 437-444.

Gu, L., Huang, Q.A., & Qin, M. (2004). A Novel Capacitive-Type Humidity Sensor Using CMOS Fabrication Technology, Sensor. Sensors and Actuators, B: Chemical, 99(2-3), 491-498.

Guo, S.Z., Gosselin, F., Guerin, N., Lanouette, A.M., Heuzey, M.C., & Therriault, D. (2013). Solvent-Cast Three-Dimensional Printing of Multifunctional Microsystems, Small, 9(24), 4118–4122.

Guo, S.Z., Heuzey, M.C., & Therriault, D. (2014). Properties of Polylactide Inks for Solvent Cast Printing of Three-Dimensional Freeform Microstructures, Langmuir, 30(4), 1142-1150.

Hawkeye, M.M., & Brett, M.J. (2011). Optimized Colorimetric Photonic-Crystal Humidity Sensor Fabricated Using Glancing Angle Deposition, Advanced Functional Materials, 21(19), 3652-3658.

Hirayama, K., Takayama, K., Haruta, S., Ishibashi, H., & Takeuchi, I. (2017). Effect of Low Concentrations of Irgarol 1051 on RGB (R, red; G, green; B, blue) Colour Values of the Hard-Coral Acropora tenuis, Marine Pollution Bulletin, 124(2), 678–686.

Hoidy, W.H., Al-Mulla, E.A.J., & Al-Janabi, K.W. (2010). Mechanical and Thermal Properties of PLLA/PCL Modified Clay Nanocomposites, The Journal of Polymers and the Environment, 18(4), 608-616.

Huang, W., Jiang, Y., Li, X., Li, X., Wang, J., Wu, Q., & Liu, X. (2013). Solvothermal Synthesis of Microporous, Crystalline Covalent Organic Framework Nanofibers and Their Colorimetric Nanohybrid Structures, ACS Applied Materials & Interfaces, 5(18), 8845-8849.

Jompang, L., Thumsorn, S., On, J.W., Surin, P., Apawet, C., Chaichalermwong, T., Kaabbuathong, N., O-Charoen, N., & Srisawat, N. (2013). Effect of Epoxidized Palm Oil on the Mechanical and Morphological Properties of a PLA–PCL Blend, Research on Chemical Intermediates, 40(2), 689-698.

578 Kim, E., Kim, S.Y., Jo, G., Kim, S., & Park, M.J. (2012). Colorimetric and Resistive Polymer
579 Electrolyte Thin Films for Real Time Humidity Sensors, ACS Applied Materials &
580 Interfaces, 4(10), 5179-5187.
581 Lalita, J., Supaphorn, T., Jessada, O.W., Prayoon, S., Chiyaprek, A., Tirapong, C., Narin, K.,
582 Narongchai, O., & Natee, S. (2013). Poly(lactic acid) and Poly(butylene succinate) Blend
583 Fibers Prepared by Melt Spinning Technique, Energy Procedia, 34, 493-499.
584 Li, F.C., Zhang, S.D., Liang, J.Z., & Wang, J.Z. (2015). Effect of Polyethylene Glycol on the
585 Crystallization and Impact Properties of Polylactide-Based Blends, Polymers for Advanced
586 Technologies, 26(5), 465–475.
587 Li, F.J., Liang, J.Z., Zhang, S.D., & Zhu, B. (2015). Tensile Properties of
588 Polylactide/Poly(ethylene glycol) Blends, Journal of Polymers and the Environment, 23(3),
589 407-415.
590 Mensing, J.P., Wisitsoraat, A., Tuantranont, A., & Kerdcharoen, T. (2013). Inkjet-Printed Sol–
591 Gel Films Containing Metal Phthalocyanines/Porphyrins for Opto-Electronic Nose
592 Applications, Sensors and Actuators, B: Chemical, 176, 428-436.
593 Nijenhuis, A.J., Colstee, E., Grijpma, D.W., & Pennings, A.J. (1996). High Molecular Weight
594 Poly(l-lactide) and Poly(ethylene oxide) Blends: Thermal Characterization and Physical
595 Properties, Polymer, 37(26), 5849-5857.
596 Oliveira, J.E., Moraes, E.A., Marconcini, J.M., Mattoso, L.H.C., Glenn, G.M., & Medeiros, E.S.
597 (2013). Properties of Poly(lactic acid) and Poly(ethylene oxide) Solvent Polymer Mixtures
598 and Nanofibers Made by Solution Blow Spinning, Journal of Applied Polymer Science,
599 129(6), 3672-3681.
600 Oyama H.T. (2009). Super-Tough Poly(lactic acid) Materials: Reactive Blending with Ethylene
601 Copolymer, Polymer, 50(3), 747-751.
602 Park, B.S., Song, J.C., Park, D.H., & Yoon, K.B. (2011). PLA/Chain-Extended PEG Blends with
603 Improved Ductility, Journal of Applied Polymer Science, 123(4), 2360-2367.
604 Pasut, G., Panisello, A., Folch-Puy, E., Lopez, A., Castro-Benítez, C., Calvo, M., Carbonell, T.,
605 Gracía-Gill, A., René, A., & Roselló-Catafau, J. (2016). Polyethylene Glycols: An
606 Effective Strategy for Limiting Liver Ischemia Reperfusion Injury, World Journal of
607 Gastroenterology, 22(28), 6501-6508.
608 Phetsuk, S., Molloy, R., Nalampang, K., Meepowpan, P., Topham, P.D., Tighe, B.J., &
609 Punyodom, W. (2020). Physical and Thermal Properties of L-lactide/ε-caprolactone
610 Copolymers: The Role of Microstructural Design, Polymer International, 69(3), 248–256.
611 Ruengdechawiwat, S., Siripitayananon, J., Molloy, R., Somsunan, R., Topham, P.D., & Tighe,
612 B.J. (2016). Preparation of a Poly(l-lactide-co-caprolactone) Copolymer Using a Novel
613 Tin(II) Alkoxide Initiator and Its Fiber Processing for Potential Use as an Absorbable
614 Monofilament Surgical Suture, International Journal of Polymeric Materials, 65(6), 277–
615 284.
616 Saha, D., Samal, S.K., Biswal, M., Mohanty, S., & Nayak, S.K. (2018). Preparation and
617 Characterization of PLA/PEO Blend Film: Effects of Poly(ethylene oxide) and
618 Poly(ethylene glycol) on the Properties, Polymer, 68(1), 164-172.

Sheth, M., Kumar, A., Davé, V., Gross, R.A., & Mccarthy, S.P. (1997). Biodegradable Polymer Blends of Poly(lactic acid) and Poly(ethylene glycol), Journal of Applied Polymer Science, 66(8), 1495-1505.

Suthapakti, K., Molloy, R., Punyodom, W., Nalampang, K., Leejarkpai, T., Topham, P.D., & Tighe, B.J. (2017). Biodegradable Compatibilized Poly(l-lactide)/Thermoplastic Polyurethane Blends: Design, Preparation and Property Testing, Journal of Polymers and the Environment, 26(5), 1818–1830.

Tachaphiboonsap, S. & Jarukumjorn, K. (2003). Toughness and Compatibility Improvement of Thermoplastic Starch/Poly(lactic acid) Blends, Advanced Materials Research, 747, 67-71.

Tian, E., Wang, J., Zheng, Y., Song, Y., Jiang, L., & Zhu, D. (2008). Colorful Humidity Sensitive Photonic Crystal Hydrogel, Journal of Materials Chemistry, 18(10), 1116-1122.

Tsigara, A., Mountrichas, G., Gatsouli, K., Nichelatti, A., Pispas, S., Madamopoulos, N., Vainos, N.A., Du, H.L., & Roubani-Kalantzopoulou, F. (2007). Hybrid Polymer/Cobalt Chloride Humidity Sensors Based on Optical Diffraction, Sensors and Actuators, B: Chemical, 120(2), 481-486.

Tuancharoensri, N., Ross, G.M., Mahasaranon, S., Topham, P.D., Ross, S. (2017). Ternary Blend Nanofibres of Poly(lactic acid), Polycaprolactone and Cellulose Acetate Butyrate for Skin Tissue Scaffolds: Influence of Blend Ratio and Polycaprolactone Molecular Mass on Miscibility, Morphology, Crystallinity and Thermal Properties, Polymer International, 66(11), 1463–1472.

Wang, T., Fu, H., Duan, X., & Li, Z. (2015). An Electrospun Micro/Nanofibrous Mesh Based Nontoxic Sensor for Optical Detection of High Humidity, Analytical Methods, 7(9), 3676-3679.

You, M.H., Yan, X., Zhang, J., Wang, X.X., He, X.X., Yu, M., Xin, N., & Long, Y.Z. (2017). Colorimetric Humidity Sensors Based on Electrocspun Polyamide/$CoCl_2$ Nanofibrous Membranes, Nanoscale Research Letters, 12(1), 1-8.

Yu, H., Cao, T., Zhou, L., Gu, E., Yu, D., & Jiang, D. (2006). Layer-by-Layer Assembly and Humidity Sensitive Behavior of Poly(ethyleneimine)/Multiwall Carbon Nanotube Composite Films, Sensor. Sensors & Actuators, B: Chemical, 119(2), 512-515.

Yu, H., Xy, P., Lee, D.W., & Li, X. (2013). Porous-Layered Stack of Functionalized AuNP–rGO (Gold Nanoparticles–Reduced Graphene Oxide) Nanosheets as a Sensing Material for the Micro-Gravimetric Detection of Chemical Vapor, Journal of Materials Chemistry A, 1(14), 4444-4450.